Molecular Pharmacology Fast Forward. Published on September 9, 2005 as doi:10.1124/mol.105.016360
This article has not been copyedited and formatted. The final version may differ from this version.

MOLPHARM/2005/016360

Redox regulation of Cdc25B by cell active quinolinediones.

Marni Brisson, Theresa Nguyen, Peter Wipf, Beomjun Joo, Billy W. Day, John S. Skoko, Emanuel M. Schreiber, Caleb Foster, Pallavi Bansal, and John S. Lazo

Departments of Pharmacology (M.B., T.N., J.S.S., C.F., P.B., J.S.L.), Pharmaceutical Sciences (B.W.D, E.M.S.), Chemistry, and the Center for Chemical Methodologies and Library Development (P.W., B.J.), University of Pittsburgh, Pittsburgh, PA 15261

Molecular Pharmacology Fast Forward. Published on September 9, 2005 as DOI: 10.1124/mol.105.016360
This article has not been copyedited and formatted. The final version may differ from this version.

MOLPHARM/2005/016360

Running title: Redox regulation of Cdc25B by quinolinediones

Corresponding author: John S. Lazo; Department of Pharmacology, University of Pittsburgh, E1340 Biomedical Science Tower, Pittsburgh, PA 15261-0001; Fax: 412-648-2229; Email: lazo@pitt.edu

Number of text pages: 39

Number of Tables: 2

Number of Figures: 9

Number of References: 46

Number of words in Abstract: 212

Number of words in Introduction: 781

Number of words in Discussion: 1454

Abbreviations: BSO, L-buthionine-sulfoximine; Cdk, cyclin dependent kinases; DA3003-1, 6-chloro-7-(2-morpholin-4-yl-ethylamino)-quinoline-5,8-dione; DTT, dithiolthreitol; IC_{50}, concentration of compound required for 50% inhibition; JUN1111, 7-(2-morpholin-4-yl-ethylamino)-quinoline-5,8-dione; PI, propidium iodide; PBS, phosphate buffered saline; DCF, 2',7'-dichlorodihydrofluorescein; H_2DCFDA, chloromethyl-2',7'-dichlorodihydrofluorescein diacetate, acetyl ester; ROS, reactive oxygen species; OMFP, *O*-methyl fluorescein phosphate.

Molecular Pharmacology Fast Forward. Published on September 9, 2005 as DOI: 10.1124/mol.105.016360
This article has not been copyedited and formatted. The final version may differ from this version.

MOLPHARM/2005/016360

ABSTRACT

Intracellular reduction and oxidation pathways regulate protein functionality through both reversible and irreversible mechanisms. The Cdc25 phosphatases, which control cell cycle progression, are potential subjects of oxidative regulation. Many of the more potent Cdc25 phosphatase inhibitors reported to date are quinones, which are capable of redox cycling. Accordingly, we utilized the previously characterized quinolinedione Cdc25 inhibitor, DA3003-1 (NSC 663284), and a newly synthesized congener, JUN1111 (7-(2-morpholin-4-yl-ethylamino)-quinoline-5,8-dione), to test the hypothesis that quinone inhibitors of Cdc25 regulate phosphatase activity through redox mechanisms. Like DA3003-1, JUN1111 selectively inhibited Cdc25 phosphatases *in vitro* in an irreversible, time-dependent manner and arrested cells in the G1 and G_2/M phases of the cell cycle. Notably, we demonstrated that both DA3003-1 and JUN1111 directly inhibited Cdc25B activity in cells. Depletion of glutathione increased cellular sensitivity to DA3003-1 and JUN1111, and *in vitro* Cdc25B inhibition by these compounds was sensitive to pH, catalase, and reductants (dithiothreitol and glutathione), consistent with oxidative inactivation. In addition, both DA3003-1 and JUN1111 rapidly generated intracellular reactive oxygen species. Analysis of Cdc25B by mass spectrometry revealed sulfonic acid formation on the catalytic cysteine of Cdc25B after *in vitro* treatment with DA3003-1. These results indicate that irreversible oxidation of the catalytic cysteine of Cdc25B is indeed a mechanism by which these quinolinediones inactivate this protein phosphatase.

Molecular Pharmacology Fast Forward. Published on September 9, 2005 as DOI: 10.1124/mol.105.016360
This article has not been copyedited and formatted. The final version may differ from this version.

INTRODUCTION

The Cdc25 phosphatases are a subfamily of tyrosine phosphatases, which dephosphorylate inhibitory tyrosine and threonine residues on cyclin dependent kinases (Cdk) (Lyon et al., 2002). All three human homologs of Cdc25 (Cdc25A, Cdc25B and Cdc25C) participate intimately in checkpoint regulation of the cell cycle (Lyon et al., 2002). Cdc25A and Cdc25B have been implicated in the oncogenesis of many human tumor types (Cangi et al., 2000; Galaktionov et al., 1995; Lyon et al., 2002; Oguri et al., 2003) and their overexpression is thought to promote the loss of cell cycle checkpoint control, uncontrolled cell proliferation, and genomic instability (Lyon et al., 2002). Thus, there is considerable interest in identifying potent and selective inhibitors of Cdc25 phosphatases.

The Cdc25 phosphatases contain a structural feature that distinguishes them from other protein tyrosine phosphatases (Buhrman et al., 2005). The crystal structures of the catalytic domains of Cdc25A and Cdc25B reveal a shallow and open active site pocket, making structure-specific inhibitor design difficult (Fauman et al., 1998; Reynolds et al., 1999). However, like other tyrosine-specific protein phosphatases, the Cdc25 phosphatases have the signature catalytic domain comprising –H-C-X_5-R-, where X is any amino acid (Denu et al., 1996). The pK_a of the active site cysteine residue of Cdc25B is unusually low (5.6-6.3) due to the unique polar environment created by a proximal α helix, the amides of the five X residues and the conserved arginine (Chen et al., 2000; Sohn and Rudolph, 2003). This ensures that the active site cysteine exists as a

Molecular Pharmacology Fast Forward. Published on September 9, 2005 as DOI: 10.1124/mol.105.016360
This article has not been copyedited and formatted. The final version may differ from this version.

thiolate anion to form a phosphocysteine intermediate, allowing for removal of the phosphate from the substrate (Cho et al., 1992; Guan and Dixon, 1991; Rudolph, 2002). The low pK_a of the active site cysteine makes it a potential target for endogenous and exogenous oxidants (Salmeen et al., 2003; Wang et al., 2004). Reactive oxygen species (ROS), such as H_2O_2, have been shown to directly inhibit the activity of Cdc25B phosphatase *in vitro* with a second-order rate constant for oxidation that is ~400 times and ~15 times faster than the oxidation of glutathione and PTP1B, respectively (Sohn and Rudolph, 2003).

Oxidative processes can profoundly influence both intracellular signaling and cell cycle progression (Tonks, 2005). For example, oxidative stress leads to mitotic cell arrest (Arrington et al., 2000; D'Agnillo and Alayash, 2001), which is reminiscent of the cell cycle arrest seen after addition of some Cdc25 phosphatase inhibitors (Kristjansdottir and Rudolph, 2004; Lyon et al., 2002). Addition of reducing agents (e.g. thioredoxin) or superoxide dismutase releases cells from mitotic arrest, coinciding with dephosphorylation of inhibitory tyrosine and threonine phosphates on Cdk1 (pCdk1), a known substrate for Cdc25 (Natsuyama et al., 1993). In addition, exposure of HeLa cells to H_2O_2 results in oxidation of the active site cysteine in Cdc25C and protein degradation, leading to cell cycle arrest (Savitsky and Finkel, 2002).

Several benzoquinones and fused quinones have previously been identified as potent *in vitro* Cdc25 inhibitors by high throughput *in vitro* screening (Kristjansdottir and Rudolph,

Molecular Pharmacology Fast Forward. Published on September 9, 2005 as DOI: 10.1124/mol.105.016360
This article has not been copyedited and formatted. The final version may differ from this version.

2004; Lyon et al., 2002). One of these compounds, DA3003-1 [NSC 663284 or (6-chloro-7-(2-morpholin-4-yl-ethylamino)quinoline-5,8-dione)], is believed to inhibit the Cdc25A catalytic domain through covalent adduct formation between DA3003-1 and a serine residue adjacent to the catalytic cysteine in Cdc25A. This led to arylation of DA3003-1 and release of the halogen substituent (Kerns et al., 1995; Pu et al., 2002). However, based on our current studies, covalent adduct formation may not be the sole or even the major mechanism of Cdc25B inhibition by quinones.

Previous studies with other protein tyrosine phosphatases and quinoid agents suggest that Cdc25B inhibition could be due to redox cycling of the quinones in the presence of oxygen (Koster, 1991; O'Brien, 1991; Wardman, 1990). Bova et al. (Bova et al., 2004) measured direct production of H_2O_2 by *ortho*-quinone inhibitors of protein-tyrosine phosphatase α. In addition, the active site cysteines of CD45 and protein tyrosine phosphatase 1B (PTP1B) can be irreversibly oxidized to sulfinic ($Cys\text{-}SO_2^-$) and sulfonic acid ($Cys\text{-}SO_3^-$) by quinones in the presence of oxygen, a course of action which is prevented by the addition of catalase or superoxide dismutase (Wang et al., 2004). Rudolph and colleagues (Sohn and Rudolph, 2003) have demonstrated the formation of a sulfenic acid ($Cys\text{-}SO^-$) intermediate after a brief H_2O_2 treatment of the catalytic domain of Cdc25B and, more recently, the generation of sulfinic and sulfonic acid species after longer treatments with H_2O_2 (Buhrman et al., 2005).

In the current study, we have examined the essential nature of the halogen substituent in DA3003-1 in Cdc25 inactivation and the possible role of oxidation induced by the quinolinediones. We provide the first direct evidence that quinolinediones can directly inactive Cdc25B in cells by generating ROS, causing irreversible oxidization of the catalytic cysteine of Cdc25B.

Molecular Pharmacology Fast Forward. Published on September 9, 2005 as DOI: 10.1124/mol.105.016360
This article has not been copyedited and formatted. The final version may differ from this version.

MATERIALS AND METHODS

Chemical synthesis. The preparation of DA3003-1 has been reported elsewhere (Lazo et al., 2001). To synthesize JUN1111 and JUN1120-2, we dissolved quinoline-5,8-dione (Barret and Daudon, 1990) (0.33 g, 2.1 mmol) in ethanol (20 ml) and added 4-(2-aminoethyl)-morpholine (0.27 ml, 2.1 mmol) at room temperature. The reaction mixture was stirred for 16 h and concentrated under reduced pressure. The crude residue was purified by chromatography on SiO_2 (methanol/CH_2Cl_2, 1:30) to give a ~2:3 mixture of JUN1111 and JUN1120-2 (0.36 g, 60%). Pure JUN1111 and JUN1120-2 were obtained as red solids by further chromatographic separation on SiO_2 (MeOH/CH_2Cl_2, 1:100). JUN1111 had a melting point of 180 °C (dec.); IR (neat) 3329, 2966, 2837, 1696, 1618, 1598 cm^{-1}; ^1H NMR δ 8.88 (dd, 1 H, *J* = 4.5, 1.6 Hz), 8.39 (dd, 1 H, *J* = 7.9, 1.6 Hz), 7.63 (dd, 1 H, *J* = 7.9, 4.5 Hz), 6.62 (bs, 1 H), 5.75 (s, 1 H), 3.80-3.60 (m, 4 H), 3.27-3.21 (m, 2 H), 2.69 (t, 2 H, *J* = 6.1 Hz), 2.55-2.35 (m, 4 H); ^{13}C NMR δ 181.5, 180.1, 153.0, 148.3, 146.8, 134.3, 130.8, 128.3, 100.6, 66.9 (2C), 55.5, 53.3 (2C), 38.8; MS (EI) *m/z* (relative intensity) 289 ($[M+2H]^{+\bullet}$, 1), 189 (4), 160 (2), 100 (100); HRMS (EI) *m/z* calculated for $C_{15}H_{19}N_3O_3$ ($[M+2H]^{+\bullet}$) 289.1426, found 289.1427. JUN1120-2 had a melting point of 182 °C (dec.); IR (neat) 3293, 2945, 2837, 1685, 1588, 1562, 1490 cm^{-1}; ^1H NMR δ 8.97 (dd, 1 H, *J* = 4.8, 1.6 Hz), 8.33 (dd, 1 H, *J* = 8.0, 1.6 Hz), 7.55 (dd, 1 H, *J* = 8.0, 4.8 Hz), 6.53 (bs, 1 H), 5.87 (s, 1 H), 3.80-3.60 (m, 4 H), 3.27-3.18 (m, 2 H), 2.69 (t, 2 H, *J* = 6.0 Hz), 2.55-2.35 (m, 4 H); ^{13}C NMR δ 181.5, 181.2, 155.1, 149.3, 147.6, 134.2, 127.4, 126.3, 102.1, 66.9 (2C), 55.5, 53.2 (2C), 38.4; MS (EI) *m/z* (relative intensity) 289 ($[M+2H]^{+\bullet}$, 2), 261 (2), 100 (75), 91 (100); HRMS (EI) *m/z* calculated for $C_{15}H_{19}N_3O_3$ ($[M+2H]^{+\bullet}$) 289.1426, found 289.1429.

Molecular Pharmacology Fast Forward. Published on September 9, 2005 as DOI: 10.1124/mol.105.016360
This article has not been copyedited and formatted. The final version may differ from this version.

***In vitro* enzyme assays.** Epitope-tagged $His_6Cdc25A_1$, $His_6Cdc25B_2$, and GST-$Cdc25C_1$ were expressed in *E. coli* and purified by Ni-NTA (His_6) or glutathione Sepharose resin (GST) as previously described (Lazo et al., 2001). Human recombinant VHR and PTP1B were purchased from BIOMOL (Plymouth Meeting, PA). A serine to alanine point mutation in the $Cdc25B_2$ catalytic domain cDNA at Ser^{450} (Acc. No. NM_021872) was accomplished using the Stratagene QuikChange Site-Directed Mutagenesis Kit and complementary custom oligonucleotide primers from Invitrogen (Carlsbad, CA). The resulting DNA was sequenced by the University of Pittsburgh Core DNA Sequencing Facility to ensure proper integration of primers. Enzyme activities in the absence and presence of inhibitors were measured using the artificial substrate *O*-methyl fluorescein phosphate (Sigma, St. Louis, MO) at concentrations equal to the K_m of each enzyme and at the optimal pH for individual enzyme activity in a 96-well microtiter plate assay based on previously described methods (Lazo et al., 2001). Fluorescence emission from the product was measured after a 20 min (VHR, PTP1B) or 60 min (Cdc25) incubation period at ambient temperature with a multiwell plate reader (Cytofluor II; Applied Biosystems, Foster City, CA; excitation filter, 485 nm/20 nm bandwidth; emission filter, 530 nm/30 nm bandwidth). IC_{50} concentrations were determined using Prism 3.0 (GraphPad Software, Inc., San Diego, CA). For dithiothreitol (DTT) studies, enzyme activities for full length $Cdc25B_2$ in the absence or presence of quinones was assessed in the presence of 2-100 mM DTT in the assay buffer. The pH of the assay buffer was adjusted from pH 7.0 – 8.3 to determine the effect of pH on compound inhibition. The effect of glutathione concentration on *in vitro* inhibition was measured by the addition of 0, 5 or 10 mM glutathione to the assay buffer. For reversibility studies with inhibitors,

Molecular Pharmacology Fast Forward. Published on September 9, 2005 as DOI: 10.1124/mol.105.016360
This article has not been copyedited and formatted. The final version may differ from this version.

we used a protocol similar to a dilution method described previously (Sohn et al., 2003). $Cdc25B_2$ full-length enzyme (60 mM Tris, 2 mM EDTA, 150 mM NaCl, pH 8.0) was preincubated with ~3X the IC_{50} of each inhibitor: 3 μM DA3003-1 or 6 μM JUN1111 for 0, 5 or 20 min at room temperature. Separately, the enzyme was also incubated with the DMSO vehicle. After preincubation, the enzyme from each treatment was diluted > 10-fold and remaining enzyme activity was determined by the above-mentioned phosphatase assay using *O*-methyl fluorescein phosphate (OMFP).

Flow cytometric analysis. tsFT210 cell synchronization and flow cytometry assays were performed as previously described (Osada et al., 1997) on a FACSCalibur flow cytometer (BD Pharmingen) and data were analyzed using ModFit LT cell-cycle analysis software (Verity Software House, Topsham, ME).

Western blotting and immunoprecipitation of pCdk1. tsFT210 cells were arrested at G_2/M by incubation at 39.4 °C for 17 h. DA3003-1 (1 or 10 μM) or JUN1111 (10 or 30 μM) or DMSO vehicle was added to cells for 1 h at 32 ^{o}C. Cells were vortexed every 10 min in ice-cold lysis buffer (50 mM Tris HCl, pH 7.5, containing 250 mM NaCl, 5 mM EDTA, and 0.1% Triton X-100) supplemented with various protease and phosphatase inhibitors. Total protein concentration was determined by Bradford assay (Bio-Rad, Hercules, CA) and lysates were incubated with 50 μl of an anti-Cdc2 p34 IgG_{2A} mouse monoclonal antibody-agarose conjugate (Santa Cruz Biotechnology, Santa Cruz, CA) overnight at 4^{o}C on an orbital rocker. Immunocomplexes were washed three times in ice-cold PBS supplemented with protease and phosphatase inhibitors. Immunocomplexes were boiled in SDS electrophoresis loading buffer and supernatants were resolved on a

12% Tris-glycine gel. Proteins were transferred to a nitrocellulose membrane and blotted with anti-phospho-Cdc2 (Tyr15) rabbit polyclonal antibody (Cell Signaling Technology, Beverly, MA) for detection of hyperphosphorylated Cdk1. Membranes were stripped and reprobed with an anti-Cdk1 mouse monoclonal antibody (Santa Cruz Biotechnology) for detection of total levels of Cdk1 (loading control).

Direct inhibition of Cdc25B in HeLa cells. The pCMV-myc-Cdc25B_2 vector was constructed by subcloning Cdc25B_2 cDNA from the pQE30-H25B plasmid and subsequent ligation into the BamHI/HindIII sites of the pCMV-Tag 2-5 vector from Stratagene (La Jolla, CA). The pCMV-myc-Cdc25B_2 plasmid was expressed in HeLa cells for 24 h followed by the addition of the vehicle control (DMSO), 10 μM DA3003-1 or JUN1111 for 2 h, or 1 mM H_2O_2 for 15 min. A pCMV-myc-vector was expressed in HeLa cells and treated with DMSO as a negative control. Cells were lysed as stated above and ectopically expressed myc-Cdc25B_2 was immunoprecipitated with an agarose-conjugated mouse monoclonal anti-myc (9E10) antibody (Santa Cruz Biotechnology). The beads were washed three times in ice-cold PBS supplemented with protease inhibitors. Remaining enzyme activity was determined with an *in vitro* OMFP assay similar to methods described previously (Lazo et al., 2001). Percent inhibition was calculated using the following formula for enzyme activity in the immunoprecipitates: [100-(Cdc25B transfected cells after treatment with DA3003-1 or JUN1111 – vector transfected cells)/(Cdc25B transfected cells after treatment with DMSO – vector transfected cells)]*100%.

Glutathione reduction in tsFT210 cells. Cellular glutathione was reduced 50% in $1x10^6$ tsFT210 cells after a 24 h incubation at 32 ^oC with 50 μM L-buthionine

Molecular Pharmacology Fast Forward. Published on September 9, 2005 as DOI: 10.1124/mol.105.016360
This article has not been copyedited and formatted. The final version may differ from this version.

sulfoximine (BSO). Glutathione levels were tested using the ApoAlert Glutathione Detection Kit from BD Biosciences Clontech (Palo Alto, CA). Cells were then treated with DMSO, DA3003-1 (0.1-10 μM) or JUN1111 (1-30 μM) for 48 h followed by counting of live and dead cells by Trypan blue exclusion. Percent inhibition of cell growth at each inhibitor concentration was calculated by: 100 – [number of live cells treated with inhibitor/number of live cells treated with DMSO] x 100%. IC_{50} concentrations were determined using Prism 3.0 (GraphPad Software, Inc.).

Measurement of cellular ROS generation and calculation of reduction potential. tsFT210 cells ($1x10^6$) were suspended in phosphate buffer saline (PBS) and preloaded with chloromethyl-2',7'-dichlorodihydrofluorescein diacetate, acetyl ester (H_2DCF) dye (Molecular Probes, Eugene, OR). Cells were washed in PBS and resuspended in PBS buffer containing 3 μM PI. Cells were then treated for 10 min with DMSO, 1 mM H_2O_2 or 10 μM of DA3003-1 or JUN1111. DCF and PI fluorescence was measured by flow cytometry using the FACSCalibur flow cytometer (BD Pharmingen). The one-electron reduction potential was calculated using the quantum chemical modeling program Spartan from Wavefunction, Inc. (Irvine, CA), based on AM1/LUMO energies.

Mass Spectrometry. Recombinant $Cdc25B_2$ catalytic domain was purified as previously described in (Guan and Dixon, 1991), with one exception: the size exclusion buffer included 50 mM Tris HCl pH 7.5, containing 300 mM NaCl, 1 mM EDTA, and 1 mM DTT. Recombinant $Cdc25B_2$ catalytic domain protein in size exclusion buffer was treated with the DMSO vehicle or a 30-fold molar excess of DA3003-1 for 1 h at 25°C. An aliquot from each reaction was removed, diluted 3-fold in 1:1 H_2O-CH_3CN containing 0.1% CF_3CO_2H, mixed with an equal volume of a sinapinic acid-saturated

solution of the same solvents, spotted on a stainless steel target and analyzed by MALDI-TOF-MS in the linear mode on an Applied Biosystems Voyager DE Pro spectrometer. Another aliquot of each solution was treated with iodoacetamide, precipitated in cold acidic acetone, resuspended in loading buffer and segregated by SDS-PAGE on a 12% Tris-glycine gel with Coomassie blue staining. Bands containing the protein, as well as a band from a lane in which no protein was loaded, were excised, de-stained with dilute methanolic aqueous acetic acid, dried and treated with sequencing grade trypsin (Promega) in aqueous NH_4HCO_3 for 12 h at 37 ^oC. The gel pieces were subjected to centrifugation and the supernatant was removed and lyophilized. The digest was resuspended in 1% aqueous HCO_2H. One portion was diluted 3-fold in 1:1 H_2O-CH_3CN containing 0.1% CF_3CO_2H, mixed with an equal volume of a α-cyano-4-hydroxycinnamic acid-saturated solution of the same solvents, spotted on a stainless steel target and analyzed by MALDI-TOF-MS and MALDI-TOF/TOF-MS/MS in reflector mode on an Applied Biosystems 4700 spectrometer. The remainder of each sample was analyzed by nanoflow LC-ESI-ion trap MS^n (n = 1 or 2) on either a ThermoFinnigan LCQ DECA XP Plus or a ThermoFinnigan LTQ system with a ThermoFinnigan Surveyor LC.

Molecular Pharmacology Fast Forward. Published on September 9, 2005 as DOI: 10.1124/mol.105.016360
This article has not been copyedited and formatted. The final version may differ from this version.

RESULTS

Previous investigations with DA3003-1 proposed the potential importance of Ser^{435} (Acc. No. NM_001789) in adduct formation and halogen release from DA3003-1, resulting in Cdc25A inhibition (Pu et al., 2002). To investigate this mechanism further, we generated a S450A mutant Cdc25B construct (equivalent to Ser^{435} in Cdc25A), expressed the recombinant protein, and evaluated inhibition with DA3003-1. The Ser^{450} mutation produced no significant difference in the Cdc25B catalytic activity and remarkably, did not alter the ability of DA3003-1 to inhibit the enzyme activity *in vitro* (data not shown). In addition, we synthesized the dehalogenated congener of DA3003-1, namely JUN1111, and its regioisomer JUN1120-2 as small molecule tools (Table 1). A comparison of the IC_{50} values for all three Cdc25 isoforms for DA3003-1 and JUN1111 revealed that the chloride substituent was not essential for inhibition (Table 1). JUN1111 was slightly more selective than DA3003-1, with higher *in vitro* IC_{50} values against VHR and PTP1B. Previously, we observed a substantial reduction in inhibition with the regioisomer of DA3003-1 and proposed this reflected different steric or electrostatic effects (Lazo et al., 2001). This effect also extended to the regioisomer of JUN1111, namely JUN1120-2, which was markedly less active against the Cdc25, VHR and PTP1B phosphatases (Table 1). Although it has been suggested by others (Ham et al., 2004) that reduction potentials can be a factor in quinone-based inhibition of Cdc25 phosphatases, the potency for *in vitro* inhibition of Cdc25 did not correlate with the calculated one electron reduction potentials (E 1/7) for these compounds (Table 1). Thus, the difference in E 1/7 values between JUN1111 and JUN1120-2 (-193 mV - (-146 mV) = -47 mV) was much smaller than that between JUN1111 and DA3003-1 (-193 mV - (-78 mV) = -115 mV), though the

difference in IC_{50} values for Cdc25 phosphatases was much greater between the two regioisomers.

The halogen was also dispensable for cell cycle arrest. We previously demonstrated that DA3003-1 caused both a G_1 and G_2M arrest in tsFT210 cells, consistent with its ability to inhibit the Cdc25 family of phosphatases (Pu et al., 2002). JUN1111 also caused both G_1 (Figure 1) and G_2/M (Figure 2) phase arrest. The G_2/M arrest induced by DA3003-1 and JUN1111 coincided with Cdk1 hyperphosphorylation, further supporting cellular inhibition of Cdc25 phosphatase activity (Figure 3). Overall, JUN1111 was slightly less potent in the tsFT210 mouse cell line as compared to DA3003-1. Nonetheless, JUN1111 was more potent than DA3003-1 in inhibiting human MDA-MB-435 breast (JUN1111, IC_{50} = 0.1 μM; DA3003-1, IC_{50} = 0.5 μM) and PC-3 prostate (JUN1111, IC_{50} = 0.8 μM; DA3003-1, IC_{50} = 1 μM) cell growth.

To confirm direct cellular inhibition of Cdc25B by DA3001-1 and JUN1111, we transfected HeLa cells with a vector containing or lacking myc-Cdc25B, before treatment of cells for 2 h with DMSO vehicle, DA3003-1, or JUN1111 or a 15 min treatment with H_2O_2. Ectopically expressed Cdc25B activity was measured by immunoprecipitation of myc-Cdc25 followed by *in vitro* phosphatase assays using OMFP as a substrate. DA3003-1 and JUN1111 inhibited the etopically expressed Cdc25B in HeLa cells by 77% and 56%, respectively, which was comparable to the 73% inhibition seen with 1 mM H_2O_2 (Figure 4). The loss of cellular enzyme activity in the immunoprecipitates of

Molecular Pharmacology Fast Forward. Published on September 9, 2005 as DOI: 10.1124/mol.105.016360
This article has not been copyedited and formatted. The final version may differ from this version.

Cdc25B from cells treated with DA3003-1 and JUN1111 is consistent with either prolonged or irreversible enzyme inhibition.

Because quinones DA3003-1 and JUN1111 clearly demonstrated both *in vitro* and cellular inhibition of Cdc25B, we investigated a possible alternative mechanism of action for these compounds. Cdc25B was pre-incubated with DA3003-1 and JUN1111 with greater than three times their IC_{50} concentrations for 0, 5 and 20 min before diluting the enzyme/inhibitor mixture 10-fold and assaying for remaining enzyme activity. As illustrated in Figure 5, both DA3003-1 and JUN1111 inhibited Cdc25B enzyme activity in an irreversible, time-dependent manner.

Recent studies have suggested that Cdc25 phosphatases are potential targets for both reversible as well as irreversible oxidation (Buhrman et al., 2005; Sohn and Rudolph, 2003). In addition, quinones are known to generate ROS (Bova et al., 2004). To investigate a possible role for redox cycling in Cdc25B inhibition, we evaluated the ability of reductant concentration and pH to alter *in vitro* Cdc25 inhibition by DA3003-1 and JUN1111. Increasing the concentration of DTT from the standard concentration used in our *in vitro* assay (1-2 mM) to 100 mM did not affect Cdc25B enzyme activity (data not shown). However, the IC_{50} values for both DA3003-1 and JUN1111 increased with increasing DTT concentrations (Figure 6A). Previous studies have also shown that pH has a direct effect on increased oxygen consumption and enzyme oxidation by quinones (Molina Portela and Stoppani, 1996; Wang et al., 2004). Thus, we also tested pH

Molecular Pharmacology Fast Forward. Published on September 9, 2005 as DOI: 10.1124/mol.105.016360
This article has not been copyedited and formatted. The final version may differ from this version.

dependency on inhibition of Cdc25 phosphatase by our quinones by varying the pH of the assay buffer from 7.0 – 8.3. The difference in pH had no effect on Cdc25B enzyme activity itself (data not shown); however, the IC_{50} values for both inhibitors continuously decreased with increasing pH, resulting in the compounds being more potent at higher pH (Figure 6B).

The reducing agent glutathione also affected Cdc25B inhibition by DA3003-1 and JUN111 both *in vitro* and in cells. Concentrations of DA3003-1 (1.6 μM) and JUN1111 (3.1 μM) that would inhibit Cdc25B by ~80% were assayed in the presence of 0, 5 or 10 mM glutathione using the *in vitro* phosphatase assay. Inhibition with both compounds decreased with increasing concentrations of glutathione (Figure 7). Glutathione concentrations of ≤10 mM did not affect basal Cdc25B enzyme activity in the absence of inhibitor (data not shown). When glutathione levels were decreased by 50% in tsFT210 cells using buthionine sulfoximine (BSO), the IC_{50} values were decreased 5-fold with DA3003-1 and 4-fold with JUN1111. These data provide evidence that the presence of a cellular reducing agent like glutathione decreased the potency of DA3003-1 and JUN1111 inhibitors against Cdc25B phosphatase activity.

The above data are consistent with the hypothesis that the Cdc25 inhibition by DA3003-1 and JUN1111 could be due to oxidation via production of reactive oxygen species (ROS). To determine if H_2O_2 was involved in quinone inhibition, we added catalase (80 U/ml) to the *in vitro* phosphatase assay. Catalase completely eliminated the inhibitory activity of

Molecular Pharmacology Fast Forward. Published on September 9, 2005 as DOI: 10.1124/mol.105.016360
This article has not been copyedited and formatted. The final version may differ from this version.

DA3003-1 and JUN1111 against Cdc25B, indicating that H_2O_2 was at least one potential ROS involved in Cdc25B inhibition. To assess direct ROS production by the quinone inhibitors, we pre-loaded tsFT210 cells with dichlorodihydrofluorescein diacetate (H_2DCFDA) dye, a cell-permeant indicator of ROS. A 10 minute treatment with 10 μM DA3003-1 or JUN1111 produced a 3-fold increase in DCF fluorescence, reflecting a rapid and marked oxidative burst (Figure 8). Simultaneous staining with PI confirmed that there was no significant cell death due to compound exposure (data not shown). Therefore, both DA3003-1 and JUN1111 are capable of rapidly generating ROS in cells.

To directly test for Cdc25B oxidation by DA3003-1, we incubated the catalytic domain of $Cdc25B_2$ (residues 350-539; Acc. No. NM_021872) in the presence or absence of a 30-fold excess of the DA3003-1 quinone at 25^{o}C for 1 h followed by protein isolation and mass spectrometric analyses. Direct analysis of vehicle-treated intact protein samples by MALDI-TOF-MS in linear, positive ion detection mode showed sharp *m/z* signals for ions of 22407 and 22490 (expected $[M+H]^+$ *m/z* = 22407). The spectrum of the DA3003-1-treated protein, in contrast, had a broad, unresolved ion signal from *m/z* 22000-23600. These results suggested multiple modifications of the protein had occurred as a result of the treatment with DA3003-1. To investigate these modifications further, the protein samples were treated with iodoacetamide to block free sulfhydryls, followed by separation using SDS-PAGE, and excision of the protein band migrating at approximately 23 kDa. The protein band was digested with trypsin and the tryptic fragments analyzed by MALDI-TOF-MS and nanoflow LC-ESI-MS on an ion trap spectrometer. When compared to the vehicle-treated sample, there was a general increase

Molecular Pharmacology Fast Forward. Published on September 9, 2005 as DOI: 10.1124/mol.105.016360
This article has not been copyedited and formatted. The final version may differ from this version.

in the presence of methionine sulfoximine-containing peptides in the DA3003-1 treated protein samples. The control protein sample gave abundant ion signals from two tryptic peptides containing the iodoacetamide-blocked active site cysteine (VILIFHC^{446}*EFSSER and RVILIFHC^{446}*EFSSER, * = carbamidomethylated). Results from MALDI-TOF/TOF-MS/MS analysis of VILIFHC^{446}*EFSSER are shown in Table 2. These ion signals, as well as any others corresponding to a peptide containing carbamidomethylated Cys^{446}, were completely absent in the MALDI-TOF-MS and LC-MS profiles of the DA3003-1 treated sample. Instead, ions corresponding to three new peptides appeared with *m/z* values and corresponding MS/MS spectra entirely consistent with the conversion of Cys^{446} to its fully oxidized, sulfonic acid form (RVILIFHC^{446}‡EFSSER, VILIFHC^{446}‡EFSSERGPR and VILIFHC^{446}‡EFSSERGPRMCR, ‡ = Cys-sulfonic acid (Cys-SO_3^-)). Results from MALDI-TOF/TOF-MS/MS analysis of RVILIFHC^{446}‡EFSSER are also given in Table 2. No evidence of the addition product of DA3003-1 (e.g., DA3003-1 + protein -> protein adduct + HCl), neither with nor without aromatization of the product (Pu et al., 2002) was found in these spectra.

Molecular Pharmacology Fast Forward. Published on September 9, 2005 as DOI: 10.1124/mol.105.016360
This article has not been copyedited and formatted. The final version may differ from this version.

DISCUSSION

The physiological role of redox regulation of protein phosphatases including PTP1B, LMW phosphatases, PTEN and SHP-2 has gained considerable support (Cho et al., 2004; Lee et al., 1998; Mahadev et al., 2001; Meng et al., 2002). Mild oxidation of protein tyrosine phosphatases at low concentrations of ROS leads to reversible oxidation of the catalytic cysteine residue to sulfenic acid (Cys-SO^-), which is readily reversible by cellular reductants. Further oxidation of the catalytic cysteine to sulfinic (Cys-SO_2^-) or sulfonic acid (Cys-SO_3^-) leads to irreversible inactivation of the enzyme. This mechanism of oxidation has been demonstrated with Cdc25B upon exposure to H_2O_2 (Buhrman et al., 2005; Sohn and Rudolph, 2003). Cdc25B can be protected from irreversible oxidation through formation of the reversible sulfenic acid species followed by rapid formation of a disulfide bridge between the active-site cysteine and a neighboring, back-door cysteine residue. The oxidized sulfenic acid and the disulfide bridge forms of the enzyme can be reduced by DTT and cellular reductants, such as thioredoxin/thioredoxin reductase, with concomitant enzyme reactivation. With increased exposure or higher concentraions of ROS (H_2O_2), further oxidation of Cdc25B occurs, resulting in irreversible deactivation.

Quinoid arenes are highly electrophilic compounds that participate in redox cycling, producing ROS that can inactivate phosphatases at their active site cysteine. The most potent and selective Cdc25 inhibitors reported to date are quinones. Most appear to be irreversible inhibitors of Cdc25 phosphatases (Lyon et al., 2002), with the possible

exception of the naphthofurandione 5169131 (Brisson et al., 2004) and some indolylhydroxyquinones (Sohn et al., 2003). Interestingly, not all quinones are potent *in vitro* Cdc25 inhibitors, indicating that there is some specificity in the chemical structure of the quinones found to inhibit this enzyme. Previous studies with DA3003-1 (Pu et al., 2002) indicated that dehalogenation of the inhibitor occurred, with formation of a covalent ether adduct with a serine residue corresponding to Ser^{435} of Cdc25A (equivalent to Ser^{450} in Cdc25B). Therefore, it is interesting that in the current study, the S450A mutation in Cdc25B did not affect DA3003-1 inhibition (data not shown) and that the chlorine moiety was not obligatory for inhibition of Cdc25A, Cdc25B or Cdc25C (JUN1111, Table 1). We also saw no evidence of a covalent adduct after incubation of Cdc25B with DA3003-1 (Table 2). This difference may be due to possible alternate confirmations of the active sites between the two Cdc25 isoforms as revealed in the x-ray crystal structures (Reynolds et al., 1999). It is also possible that redox regulation and adduct formation occur under different reaction conditions. A low concentration of reducing agent is required to reduce the quinone inhibitor and initiate redox cycling and ROS production (Bova et al., 2004). In the previous investigations of adduct formation, a reductant was not included in the buffer conditions when incubating DA3003-1 with the enzyme; therefore, in the absence of redox cycling, it is possible that arylation of DA3003-1 and adduct formation was favored. Since DTT was added in the current experiment, oxidation most likely became the dominant mechanism of inhibition.

We have provided considerable experimental evidence suggesting that quinolinediones participate in redox cycling, leading to Cdc25B inactivation. First, increasing

Molecular Pharmacology Fast Forward. Published on September 9, 2005 as DOI: 10.1124/mol.105.016360
This article has not been copyedited and formatted. The final version may differ from this version.

concentrations of DTT (Figure 6A) and glutathione (Figure 7) caused a subsequent decrease in Cdc25B inhibition by DA3003-1 and JUN1111. Second, when DA3003-1 and JUN1111 were incubated with Cdc25B phosphatase in the absence of reducing agents, the quinones were not capable of inhibiting Cdc25B, presumably because redox cycling was not initiated. Therefore, the presence of high concentrations of reducing agents interfered with Cdc25B oxidation and inactivation by quinolinediones, while low reductant levels were required to induce inhibition by initiating quinone redox cycling and subsequent production of ROS. Third, the presence of catalase completely abolished inhibition by DA3003-1 and JUN1111, indicating that H_2O_2 production was important in inhibiting Cdc25B phosphatase activity. Fourth, the pH of the reaction also directly affected enzyme oxidation. Raising the reaction pH from pH 6.0 up to pH 8.0 enhances oxygen consumption by quinones, thereby, increasing the rate of oxidation of enzymes (Molina Portela and Stoppani, 1996; Wang et al., 2004). Furthermore, increasing the pH above 7.0 increases hydroquinone oxidation by superoxide, resulting in increased production of H_2O_2 (Bova et al., 2004; Ordonez and Cadenas, 1992). Thus, the IC_{50} concentrations of DA3003-1 and JUN1111 decreased with increasing pH from pH 7.0 – 8.3 (Figure 6B). Finally, we observed rapid ROS formation in cells treated with both DA3003-1 and JUN1111 (Figure 8). Although DA3003-1 appeared to participate in redox cycling in cells, cell lines differing in levels of NAD(P)H:quinone oxidoreductase-1 are equally sensitive to DA3003-1 cytotoxic effects (Han et al., 2004). Therefore, these compounds may be substrates for other quinone reductases or dehydrogenases, such as carbonyl reductase and xanthine dehydrogenase.

Molecular Pharmacology Fast Forward. Published on September 9, 2005 as DOI: 10.1124/mol.105.016360
This article has not been copyedited and formatted. The final version may differ from this version.

The oxidation caused by quinolinediones may exploit the extreme reactivity of the Cdc25 phosphatases to oxidants and their susceptibility to form higher, irreversibly oxidized sulfinic and sulfonic acid states, compared to other protein tyrosine phosphatases (PTP1B, VHR). This may be due, in part, to the open, exposed active site pocket of Cdc25 (Denu and Tanner, 1998; Reynolds et al., 1999; Rudolph, 2004). For example, the deeper active site pocket in PTP1B causes the rate of inactivation of the PTP1B to be 15-fold less than that of Cdc25B (Sohn and Rudolph, 2003). This differential reactivity provides a possible explanation for the selectivity of our quinolinediones for inhibition of Cdc25 phosphatases over VHR and PTP1B (Table 1). ROS have also been shown to oxidize and inactivate mitogen activated protein kinase phosphatases or MKPs resulting in Jun N-terminal kinase (JNK) activation (Kamata et al., 2005). Therefore, we examined the effects of DA3003-1 and JUN1111 on MKP-1 both *in vitro* and in cells. Both compounds had no effect on *in vitro* MKP-1 activity up to 100 μM. Furthermore, addition of DA3003-1 (10 μM) and JUN1111 (30 μM) to HeLa cells for 1 h did not induce activation of JNK when lysates were probed with an anti-phospho-SAPK/JNK (Thr183/Tyr185) antibody (data not shown). Although these studies indicate some selectivity of the compounds for Cdc25 phosphatases, we recognize that more of the almost 100 human protein tyrosine phosphatases would need to be evaluated to securely state a high degree of selectivity both *in vitro* and *in vivo*.

The ability of a particular quinone to redox cycle and produce ROS is dependent on the redox potential of the compound (Bova et al., 2004). Both DA3003-1 and JUN1111 were equally competent in generating cellular ROS as measured by the indicator dye DCF.

Both rapidly caused a 3-fold increase in ROS as compared to DMSO treated cells (Figure 8), which is somewhat surprising as DA3003-1 had a much higher calculated E1/7 (-78 mV) compared with JUN1111 (-193 mV). While other chemical factors such as cellular uptake or steric properties enabling docking with the targeted phosphatase (Lazo et al., 2002) could be important, both compounds are sufficiently close to the one-electron reduction potential of oxygen (-155 mV) to generate significant amounts of superoxide.

We have provided direct evidence of irreversible inactivation and oxidation of Cdc25B after exposure to DA3003-1. DA3003-1 and JUN1111 irreversibly inactivated Cdc25B enzyme activity in a time-dependent manner, similar to inactivation seen with H_2O_2 (Figure 4, 5). Mass spectrometry analysis of the Cdc25B catalytic domain after a one hour *in vitro* incubation with DA3003-1 revealed that the catalytic cysteine was irreversibly oxidized to sulfonic acid (Figure 9, Table 2). Figure 9 shows the fragmentation patterns of the tryptic peptide containing the iodoacetamide-blocked active site cysteine (* = carbamidomethylated) as well as the DA3003-1 treated peptide that revealed the oxidized catalytic cysteine (‡ = Cys-sulfonic acid). A total of seven fragments, as well as an interal ion fragment – H_2O of mass 584 (Table 2), confirmed an increase in mass coinciding with conversion of the catalytic cysteine to its sulfonic acid form. These data are in agreement with irreversible oxidation of the catalytic cysteines of other phosphatases by *ortho*- and *para*-quinone inhibitors producing ROS (Bova et al., 2004; Wang et al., 2004). We recognize that additional posttranslational modifications, such as S-glutathionylation, may regulate Cdc25 phosphatase activity as seen with

regulation of PTP1B (Barrett et al., 1999). This possibility should be addressed in future studies.

In conclusion, the *in vitro* inhibition of Cdc25B by *para*-quinolinediones DA3003-1 and JUN1111 appears to be at least in part due to ROS production and irreversible oxidation of the catalytic cysteine thiol to sulfonic acid. Differences in Cdc25 phosphatase inhibition are not directly correlated to the redox potentials of quinones, allowing for the possibility that interactions controlled by steric and electronic factors may confer some specificity for inhibition. Future synthesis of analogs of the quinolinediones to promote selective inhibition of Cdc25 could entail the addition of moieties that would better direct the generated ROS to the active site of Cdc25.

Molecular Pharmacology Fast Forward. Published on September 9, 2005 as DOI: 10.1124/mol.105.016360
This article has not been copyedited and formatted. The final version may differ from this version.

MOLPHARM/2005/016360

ACKNOWLEDEMENTS

We would like to thank Johannes Rudolph at the Duke University Medical Center for generously providing the $Cdc25B_2$ catalytic domain construct that we used for our spectrometry analysis and for his helpful advice.

REFERENCES

Arrington ED, Caldwell MC, Kumaravel TS, Lohani A, Joshi A, Evans MK, Chen HT, Nussenzweig A, Holbrook NJ and Gorospe M (2000) Enhanced sensitivity and long-term G2 arrest in hydrogen peroxide-treated Ku80-null cells are unrelated to DNA repair defects. *Free Radic. Biol. Med.* **29**:1166-1176.

Barret R and Daudon M (1990) Oxidation of phenols to quinones by bis(trifluoroacetoxy)iodobenzene. *Tetrahedron Lett.* **31**:4871-4872.

Barrett WC, DeGnore JP, Konig S, Fales HM, Keng YF, Zhang ZY, Yim MB and Chock PB (1999) Regulation of PTP1B via glutathionylation of the active site cysteine 215. *Biochemistry* **38**:6699-6705.

Bova MP, Mattson MN, Vasile S, Tam D, Holsinger L, Bremer M, Hui T, McMahon G, RIce A and Fukuto JM (2004) The oxidative mechanism of action of *ortho*-quinone inhibitors of protein-tyrosine phosphatase α is mediated by hydrogen peroxide. *Arch. Biochem. Biophys.* **429**:30-41.

Brisson M, Nguyen T, Vogt A, Yalowich J, Giorgianni A, Tobi D, Bahar I, Stephenson CR, Wipf P and Lazo JS (2004) Discovery and characterization of novel small molecule inhibitors of human Cdc25B dual specificity phosphatase. *Molec. Pharmacol.* **66**:824-833.

Buhrman G, Parker B, Sohn J, Rudolph J and Mattos C (2005) Structural mechanism of oxidative regulation of the phosphatase Cdc25B via an intramolecular disulfide bond. *Biochemistry* **44**:5307-5316.

Cangi MG, Cukor B, Soung P, Signoretti S, Moreira JG, Ranashinge M, Cady B, Pagano M and Loda M (2000) Role of Cdc25A phosphatase in human breast cancer. *J. Clin. Invest.* **106**:753-761.

Chen W, Wilborn M and Rudolph J (2000) Dual-specific Cdc25B phosphatase: in search of the catalytic acid. *Biochemistry* **39**:10781-10789.

Cho H, Krishnaraj R, Kitas E, Bannwarth W, Walsh CT and Anderson KS (1992) Isolation and structural elucidation of a novel phophocysteine intermediate in the LAR protein tyrosine phosphatse enzymatic pathway. *J. Amer. Chem. Soc.* **114**:7296-7298.

Cho S-H, Lee C-H, Ahn Y, Kim H, Kim H, Ahn C-Y, Yang K-S and Lee S-R (2004) Redox regulation of PTEN and protein tyrosine phosphatases in H_2O_2-mediated cell signaling. *FEBS Letters* **560**:7-13.

D'Agnillo F and Alayash AI (2001) Redox cycling of diaspirin cross-linked hemoglobin induces G2/M arrest and apoptosis in cultured endothelial cells. *Blood* **98**:3315-3323.

Denu JM, Stuckey JA, Saper MA and Dixon JE (1996) Form and function in protein dephosphorylation. *Cell* **87**:361-364.

Denu JM and Tanner JW (1998) Specific and reversible inactivation of protein tyrosine phosphatases by hydrogen peroxide: evidence for a sulfenic acid intermediate and implications for redox regulation. *Biochemistry* **37**:5699-5642.

Fauman EB, Cogswell JP, Lovejoy B, Rocque WJ, Holmes W, Montana VG, Piwnica-Worms H, Rink MJ and Saper MA (1998) Crystal structure of the catalytic domain of the human cell cycle control phosphatase, Cdc25A. *Cell* **93**:617-625.

Galaktionov K, Lee AK, Eckstein J, Draetta G, Meckler J, Loda M and Beach D (1995) CDC25 phosphatases as potential human oncogenes. *Science* **269**:1575-7.

Guan KL and Dixon JE (1991) Evidence for protein-tyrosine-phosphatase catalysis proceeding via a cysteine-phosphate intermediate. *J. Biol. Chem.* **266**:17026-17030.

Ham SW, Choe J-I, Wang M-F, Peyregne V and Carr BI (2004) Florinated quinoid inhibitor: possible 'pure' arylator predicted by the simple theoretical calculation. *Bioorg. Med. Chem. Ltrs.* **14**:4103-4105.

Han Y, Shen H, Carr BI, Wipf P, Lazo JS and Pan SS (2004) NAD(P)H:quinone oxidoreductase-1-dependent and -independent cytotoxicity of potent quinone Cdc25 phosphatase inhibitors. *J. Pharmacol. Expt. Therap.* **309**:64-70.

Kamata H, Honda S, Maeda S, Chang L, Hirata H and Karin M (2005) Reactive oxygen species promote TNFalpha-induced death and sustained JNK activation by inhibiting MAP kinase phosphatases. *Cell* **120**:649-661.

Kerns J, Naganathan S, Dowd P, Finn FM and Carr B (1995) Thioalkyl derivatives of vitamin K_3 and vitamin K_3 oxide inhibit growth of Hep3B and HepG2 cells. *Bioorg. Chem.* **23**:101-108.

Koster AS (1991) Bioreductive activation of quinones: a mixed blessing. *Pharm. Weekbl. Sci.* **13**:123-126.

Kristjansdottir K and Rudolph J (2004) Cdc25 Phosphatases and Cancer. *Chemistry and Biology* **11**:1043-1051.

Lazo JS, Aslan DC, Southwick EC, Cooley KA, Ducruet AP, Joo B, Vogt A and Wipf P (2001) Discovery and biological evaluation of a new family of potent inhibitors of the dual specifity protein phosphatase Cdc25. *J. Med. Chem.* **44**:4042-4049.

Lazo JS, Nemoto K, Pestell KE, Cooley K, Southwick EC, Mitchell DA, Furey W, Gussio R, Zaharevitz DW, Joo B and Wipf P (2002) Identification of a potent and selective pharmacophore for Cdc25 dual specificity phosphatase inhibitors. *Molec. Pharmacol.* **61**.

Lee SR, Kwon KS, Kim SR and Rhee SG (1998) Reversible inactivation of protein-tyrosine phosphatase 1B in A431 cells stimulated with epidermal growth factor. *J. Biol. Chem.* **273**:15366-15372.

Lyon MA, Ducret AP, Wipf P and Lazo JS (2002) Dual-specificity phosphatases as targets for antineoplastic agents. *Nature Rev. Drug Discov.* **1**:961-976.

Mahadev K, Zilbering A, Zhu L and Goldstein BJ (2001) Insulin-stimulated hydrogen peroxide reversibly inhibits protein-tyrosine phophatase 1B in vivo and enhances the early insulin action cascade. *J. Biol. Chem.* **276**:21938-21942.

Meng TC, Fukada T and Tonks NK (2002) Reversible oxidation and inactivation of protein tyrosine phosphatases in vivo. *Mol. Cell* **9**:387-399.

Molina Portela MP and Stoppani AOM (1996) Redox cycling of β-lapachone and related *o*-naphthoquinones in the presence of dihydrolipoamide and oxygen. *Biochem. Pharm.* **51**:275-283.

Natsuyama S, Noda Y, Yamashita M, Nagahama Y and Mori T (1993) Superoxide dismutase and thioredoxin restore defective p34cdc2 kinase activation in mouse two-cell block. *Biochim. Biophys. Acta* **1176**:90-94.

O'Brien PJ (1991) Molecular mechanisms of quinone cytotoxicity. *Chem. Biol. Interact.* **80**:1-41.

Oguri T, Singh SV, Nemoto K and Lazo JS (2003) The carinogen (7*R*,8*S*)-dihydroxy-(9*S*,10*R*)-epoxy-7,8,9,10-tetrahydrobenzo[*a*]pyrene induces Cdc25B expression in human bronchial and lung cancer cells. *Cancer Res.* **63**:771-775.

Ordonez ID and Cadenas E (1992) Thiol oxidation coupled to DT-diaphorase-catalysed reduction of diaziquone. Reductive and oxidative pathways of diaziquone semiquinone modulated by glutathione and superoxide dismutase. *Biochem J.* **286**:481-490.

Osada H, Cui CB, Onose R and Hanaoka F (1997) Screening of cell cycle inhibitors from microbial metabolites by a bioassay using a mouse cdc2 mutant cell line, tsFT210. *Bioorg. Med. Chem.* **5**:193-203.

Pu L, Amoscato AA, Bier ME and Lazo JS (2002) Dual G1 and G2 phase inhibition by a novel, selective Cdc25 inhibitor 7-chloro-6-(2-morpholin-4-ylethylamino)-quinoline-5,8-dione. *J. Biol. Chem.* **277**:46877-46885.

Reynolds RA, Yem AW, Wolfe CL, Deibel M, Chidester CG and Watenpaugh KD (1999) Crystal structure of the catalytic subunit of Cdc25B required for G2/M phase transition of the cell cycle. *J. Mol. Biol.* **293**:559-568.

Rudolph J (2002) Catalytic mechanism of Cdc25. *Biochemistry* **41**:14613-14623.

Rudolph J (2004) Targeting the Neighbor's Pool. *Mol Pharmacol* **66**:780-782.

Salmeen A, Andersen JN, Myers MP, Meng TC, Hinks JA, Tonks NK and Barford D (2003) Redox regulation of protein tyrosine phosphatase 1B involves a sulphenyl-amide intermediate. *Nature* **423**:769-773.

Savitsky PA and Finkel T (2002) Redox Regulation of Cdc25C. *J. Biol. Chem.* **277**:20535-20540.

Sohn J, Kiburz B, Li Z, Deng L, Safi A, Pirrung MC and Rudolph J (2003) Inhibition of Cdc25 phosphatases by indoyldihyroxyquinones. *J. Med. Chem.* **46**:2580-2588.

Sohn J and Rudolph J (2003) Catalytic and Chemical Competence of Regulation of Cd25 Phosphatase by Oxidation/Reduction. *Biochemistry* **42**:10060-10070.

Takemasa I, Yamamoto H, Sekimoto M, Ohue M, Noura S, Miyake Y, Matsumoto T, Aihara T, Tomita N, Tamaki Y, Sakita I, Kikkawa N, Matsuura N, Shiozaki H and Monden M (2000) Overexpression of CDC25B phosphatase as a novel marker of poor prognosis of human colorectal carcinoma. *Cancer Res.* **60**:3043-3050.

Tonks NK (2005) Redox redux: revisiting PTPs and the control of cell signaling. *Cell* **121**:667-670.

Wang Q, Dube D, Friesen RW, LeRiche TG, Bateman KP, Trimble L, Sanghara, Pollex R, Ramachandran C, Gresser MJ and Huang Z (2004) Catalytic inactivation of protein tyrosine phosphatase CD45 and protein tyrosine phosphatase 1B by polyaromatic quinones. *Biochemistry* **43**:4294-4303.

Wardman P (1990) Bioreductive activation of quinones: redox properties and thiol reactivity. *Free Radic. Res. Commun.* **8**:219-229.

Molecular Pharmacology Fast Forward. Published on September 9, 2005 as DOI: 10.1124/mol.105.016360
This article has not been copyedited and formatted. The final version may differ from this version.

MOLPHARM/2005/016360

FOOTNOTES

This work was supported in part by U. S. Public Health Service National Institutes of Health Grants CA78039 and GM06585 and the Fiske Drug Discovery Fund.

Brisson, M**,** Nguyen, T, Wipf, P, Joo, B, Day, BW, Schreiber, EM, Skoko, JS, Foster, C, Bansal, P and Lazo, JS. (2005). Redox regulation of Cdc25B by novel cell active quiolinediones. *AACR Abstract.* **660**: 107.

To whom request for reprints should be addressed: Department of Pharmacology, University of Pittsburgh, E1340 Biomedical Science Tower, Pittsburgh, PA 15261-0001; Email: lazo@pitt.edu

Molecular Pharmacology Fast Forward. Published on September 9, 2005 as DOI: 10.1124/mol.105.016360
This article has not been copyedited and formatted. The final version may differ from this version.

FIGURE LEGENDS

Figure 1. G_1 phase arrest with DA3003-1 and JUN1111. tsFT210 cells were cultured at the permissive temperature of 32 ^{o}C and then incubated at the nonpermissive temperature (39.4^{o}C) for 17 h to synchronize cells at G_2/M. Cells were then released for 4-6 h at 32 ^{o}C to arrest cells at the G_1 checkpoint. DMSO or inhibitor was added for an additional 6 h at 32 ^{o}C. Panel A. Asynchronous control. Panel B. G_2/M arrested cells after temperature shift for 17 h at 39.4 ^{o}C. Panel C. G_1 arrested cells after temperature shift back to 32^{o}C. Panel D. DMSO treated cells. Panel E. Cells treated with 50 μM roscovitine (positive control). Panel F. Cells treated with 10 μM DA3003-1. Panel G & H. Cells treated with 10 μM or 30 μM JUN1111. Data are representative of three independent experiments.

Figure 2. G_2/M arrest with DA3003-1 and JUN1111. tsFT210 cells were cultured at the permissive temperature of 32 ^{o}C and then incubated for 17 h at the nonpermissive temperature (39.4 ^{o}C). DMSO or drug was added to cells for an additional 6 h at 32 ^{o}C. Panel A. Asynchronous control. Panel B. G_2/M arrested cells after temperature shift for 17 h at 39.4 ^{o}C. Panel C. DMSO treated cells. Panel D. Cells treated with 1 μM nocodazole (positive control). Panel E. Cells treated with 10 μM DA3003-1. Panel F & G. Cells treated with 10 μM or 30 μM JUN1111. Data are representative of three independent experiments.

Molecular Pharmacology Fast Forward. Published on September 9, 2005 as DOI: 10.1124/mol.105.016360
This article has not been copyedited and formatted. The final version may differ from this version.

Figure 3. Cdk1 is hyperphosphorylated in the presence of DA3003-1 and JUN1111. G_2/M arrested tsFT210 cells were released for 1 h in the presence of 10 μM and 30 μM of JUN1111 or 1 μM and 10 μM of DA3003-1 or DMSO vehicle followed by immunoprecipitation with anti-Cdk1 mouse monoclonal antibody. Western blots were probed with phospho-Cdk1 (Tyr15) antibody. Blots were stripped and reprobed with total Cdk1 antibody as a loading control.

Figure 4. DA3003-1 and JUN1111 directly inhibit transfected Cdc25B in HeLa cells. Transfected cells were treated with DA3003-1 (10 μM), JUN1111 (10 μM) or H_2O_2 (1 mM) followed by immunoprecipitation of myc-Cdc25B. The remaining enzyme activity was tested *in vitro* using OMFP as a substrate. Percent inhibition was calculated by comparing to DMSO treated myc-Cdc25B transfected cells (positive control) and DMSO treated myc-vector transfected cells (negative control). Results are mean ± SEM (n = 4).

Figure 5. DA3003-1 and JUN1111 are irreversible inhibitors of Cdc25B. Recombinant Cdc25B was pre-incubated with ~3 x the IC_{50} of DA3003-1 (2.5 μM) or JUN1111 (6 μM) for 0, 5 or 20 min in the absence of substrate and then diluted ten fold and assayed for enzyme activity. Results are mean ± SEM (n = 3). Statistical significance was assessed by one-way ANOVA. ***$p<0.001$ compared to DMSO control.

Molecular Pharmacology Fast Forward. Published on September 9, 2005 as DOI: 10.1124/mol.105.016360
This article has not been copyedited and formatted. The final version may differ from this version.

Figure 6. Effect of DTT concentration and pH on phosphatase inhibition. Panel A. Cdc25B phosphatase inhibition by DA3003-1 and JUN1111 was tested using our *in vitro* enzyme assay as described in Materials and Methods at DTT concentrations of 2, 10, 25 and 100 mM. Results are mean ± SEM ($n \geq 3$). Panel B. Cdc25B phosphatase inhibition by DA3003-1 and JUN1111 was tested using our *in vitro* enzyme assay as described in Materials and Methods under various pH conditions (pH 7 – 8.3). Results are mean ± SEM (n = 3). IC_{50} values were calculated using Graph Pad Prism software. A positive correlation of +1 (effect of DTT on IC_{50}) and a negative correlation of -1 (effect of pH on IC_{50}) were determined by Spearman's Rank Correlation.

Figure 7. Glutathione decreases the potency of DA3003-1 and JUN1111. *In vitro* inhibition of Cdc25B phosphatase by DA3003-1 (1.56 μM) and JUN1111 (3.13 μM) was tested in the presence of increasing concentrations of glutathione (0, 5 and 10 mM). Results are mean ± SEM (n = 6). A negative correlation of -1 (effect of glutathione on % inhibition of enzyme) was determined by Spearman's Rank Correlation.

Figure 8. DA3003-1 and JUN1111 produce reactive oxygen species (ROS) in cells. tsFT210 cells were preloaded with DCF dye (to measure ROS) and propidium iodide (to measure cell death) before treatment with DMSO, DA3003-1 (10 μM) or JUN1111 (10 μM) for 10 min. Resulting DCF and PI fluorescence was measured by flow cytometry. Results are mean ± SEM (n = 3). Statistical significance was assessed by one-way ANOVA. ***$p<0.001$ compared to DMSO control.

Molecular Pharmacology Fast Forward. Published on September 9, 2005 as DOI: 10.1124/mol.105.016360
This article has not been copyedited and formatted. The final version may differ from this version.

Figure 9. Fragmentation patterns for peptides generated from tryptic digests of $Cdc25B_2$ incubated with DMSO vehicle or with a 30-fold molar excess of DA3003-1 for MALDI-TOF-MS spectra analysis. RVILIFHC^{446}‡EFSSER (‡ = Cys-sulfonic acid) treated with DA3003-1. VILIFHC^{446}*EFSSER (* = carbamidomethylated) containing the iodoacetamide-blocked active site cysteine.

Molecular Pharmacology Fast Forward. Published on September 9, 2005 as DOI: 10.1124/mol.105.016360
This article has not been copyedited and formatted. The final version may differ from this version.

MOLPHARM/2005/016360

Table 1. Chemical structures and IC_{50} values for the quinolinediones assayed against Cdc25A, Cdc25B, Cdc25C, VHR, and PTP1B. Results are mean ± SEM (n = 4). The one-electron reduction potential (E1/7) was calculated using a quantum chemical modeling program as described in the Material and Methods Section.

		IC_{50} (μM)					
Name	**Structure**	**Cdc25A**	**Cdc25B**	**Cdc25C**	**VHR**	**PTP1B**	**E 1/7 (mV)**
DA3003-1	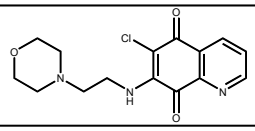	0.50 ± 0.01	0.91 ± 0.36	0.47 ± 0.09	10 ± 0.2	15 ± 0.3	-78
JUN1111	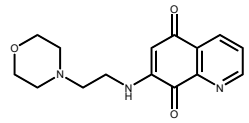	0.38 ± 0.06	1.8 ± 0.7	0.66 ± 0.27	28 ± 1.7	37 ± 0.2	-193
JUN1120-2	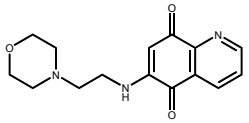	3.0 ± 0.05	20 ± 8.1	16 ± 0.48	320 ± 9.8	370 ± 23	-146

Molecular Pharmacology Fast Forward. Published on September 9, 2005 as DOI: 10.1124/mol.105.016360
This article has not been copyedited and formatted. The final version may differ from this version.

Table 2. Collision-induced dissociation fragment ions from 1 kV MALDI-TOF/TOF-MS/MS experiments on the $[M+H]^+$ ions containing the active site cysteine seen in the MALDI-TOF-MS spectra of tryptic digests from $Cdc25B_2$ incubated with DMSO or with a 30-fold molar excess of DA3003-1.

RVILIFHC(SO_3)EFSSER (*m/z* found 1783.8821, expected 1783.8801)				**carbamidomethylated-VILIFHCEFSSER (*m/z* found 1636.8134, expected 1636.8157)**		
Ion signal observed (*m/z*) [a]	**Ion type**	**Expected *m/z***		**Ion signal observed (*m/z*)** [a]	**Ion type**	**Expected *m/z***
70.081	R immonium	70.07		70.084	R immonium	70.07
72.088	V immonium	72.08		72.079	V immonium	72.08
157.071	SS-H_2O	157.06		158.079	y_1-NH_3	158.09
175.065	SS internal (or y_1)	175.07 (or 175.12)		175.066	SS internal (or y_1)	175.07 (or 175.12)
304.145	y_2	304.16		304.149	y_2	304.16
369.287	b_3	369.26		326.313	b_3	326.24
584.163	C(SO_3)EFSS – H_2O	584.17		391.214	y_3	391.19
595.464	b_5	595.43		439.312	b_4	439.33
625.306	y_5	625.29		625.298	y_5	625.29
742.513	b_6	742.5		754.513	y_6	754.34
879.568	b_7	879.56		914.488	y_7	914.37
905.326	y_7	905.33		1051.511	y_8	1051.43
1030.59	b_8	1030.55		1198.631	y_9	1198.5
1189.501	y_9	1189.46		1311.578	y_{10}	1311.58
1302.524	y_{10}	1302.54		1425.002	y_{11}	1424.66
1415.707	y_{11}	1415.63		1537.699	y_{12}	1537.75
1510.719	y_{12}-H_2O	1510.7				
1528.814	y_{12}	1528.71				
1627.821	y_{13}	1627.78				

[a]Averaged from 3000 MS/MS spectra.

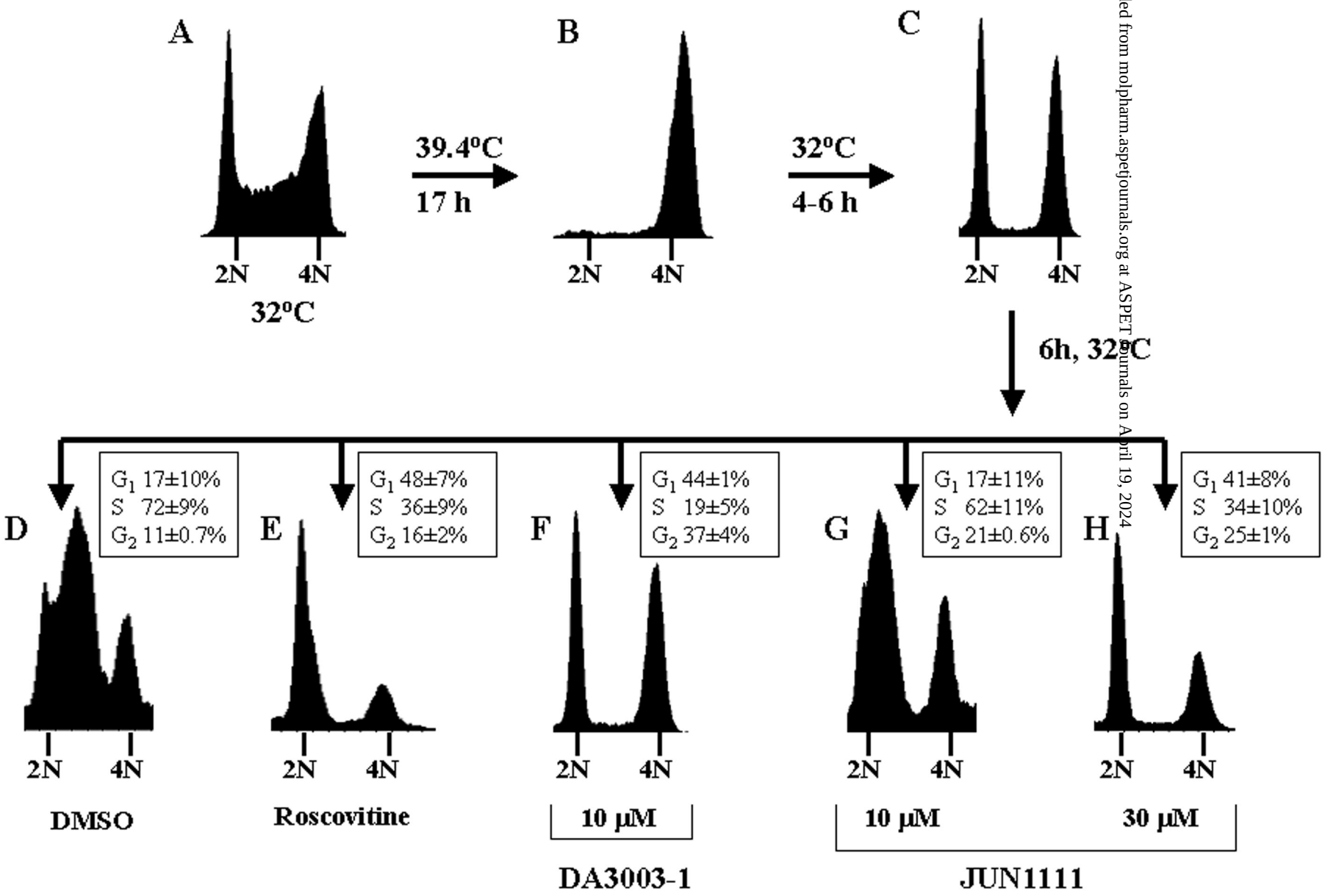

Figure 1

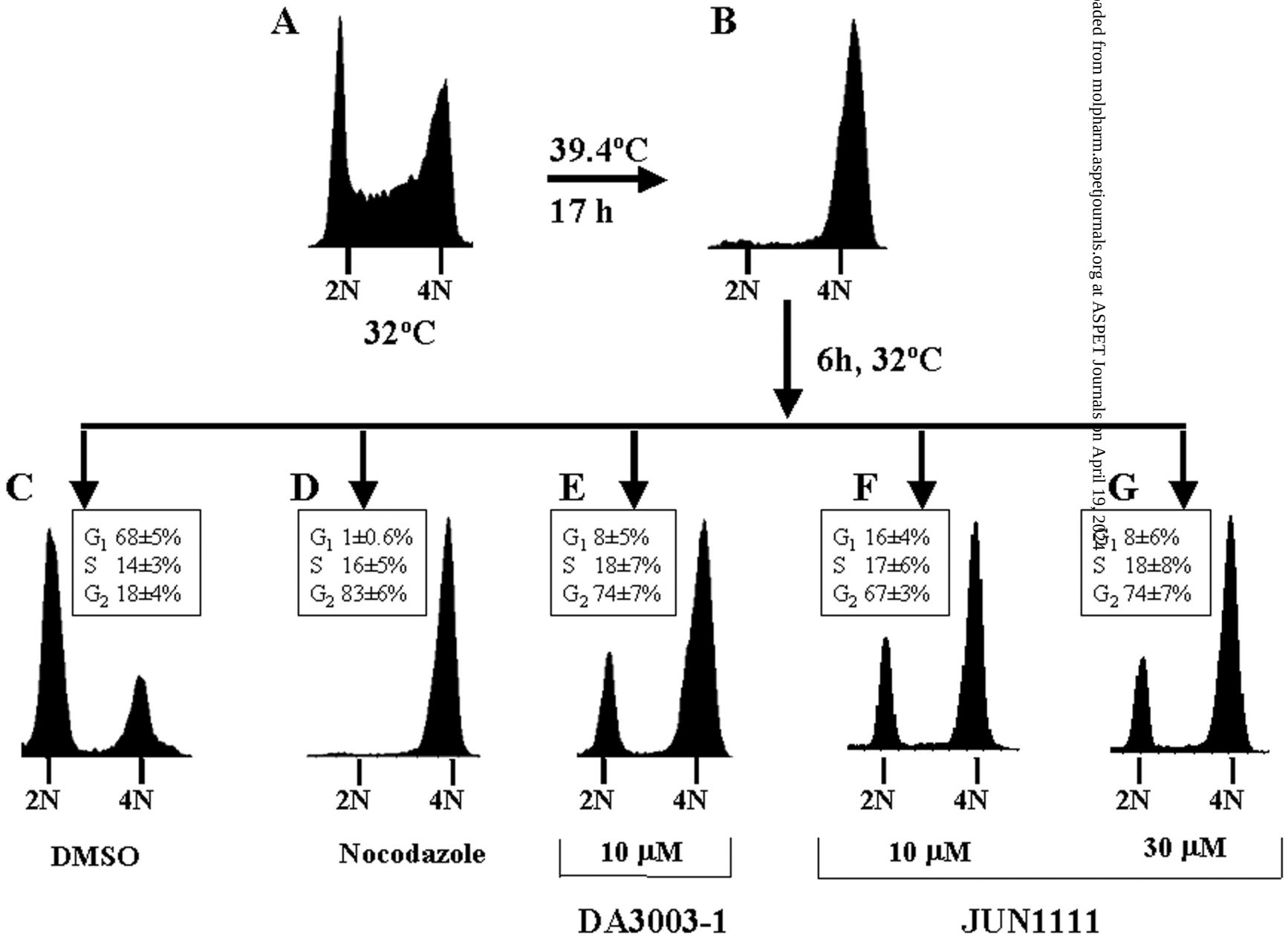

Figure 2

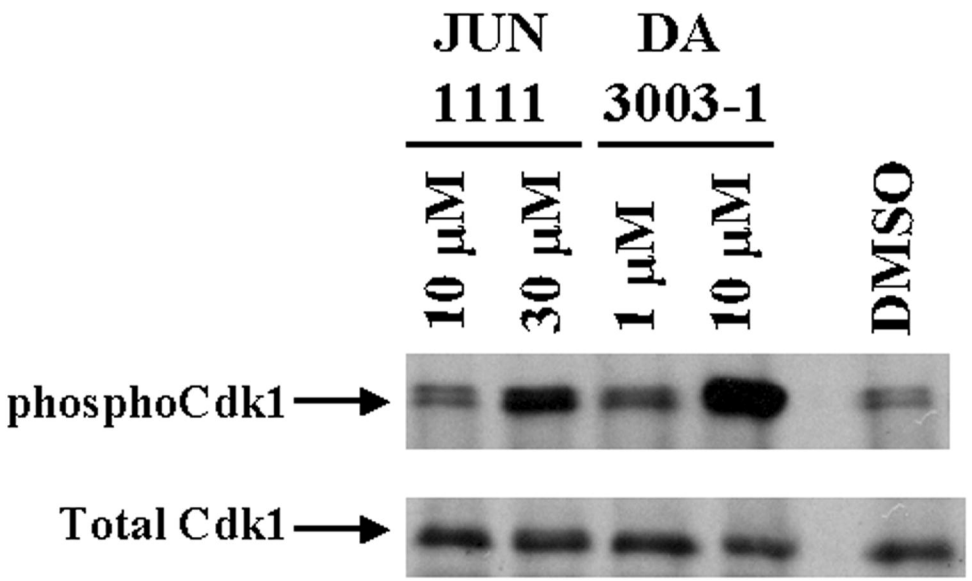

Figure 3

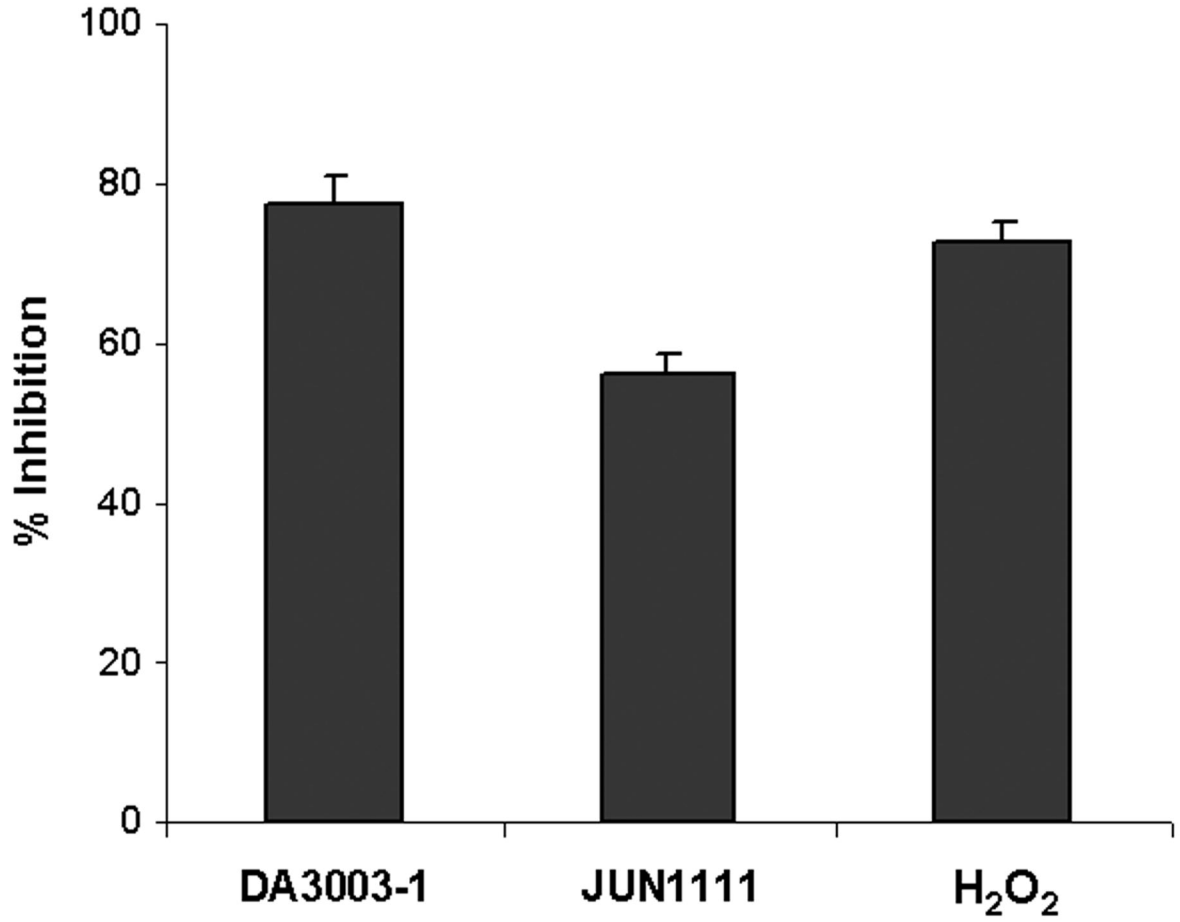

Figure 4

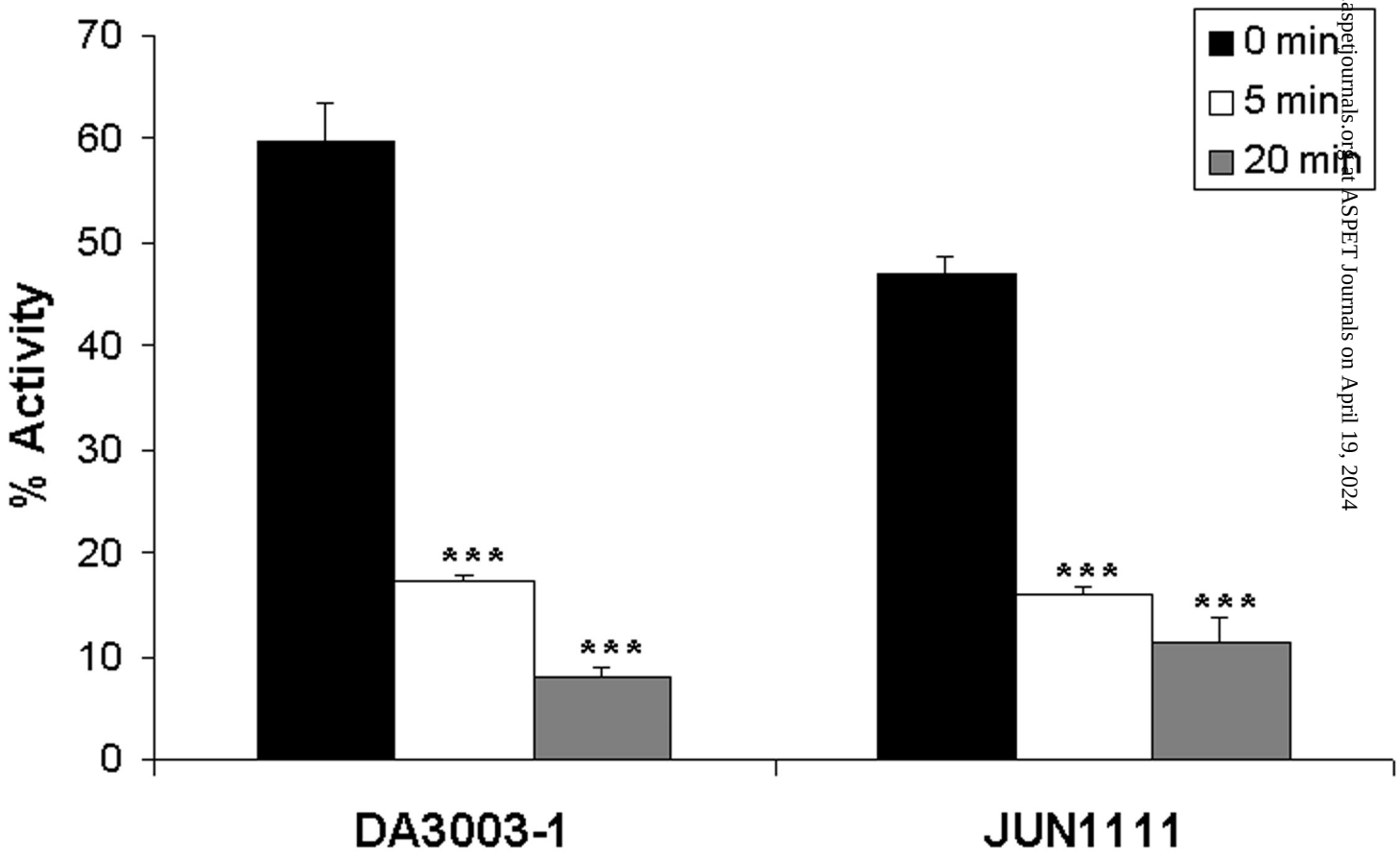

Figure 5

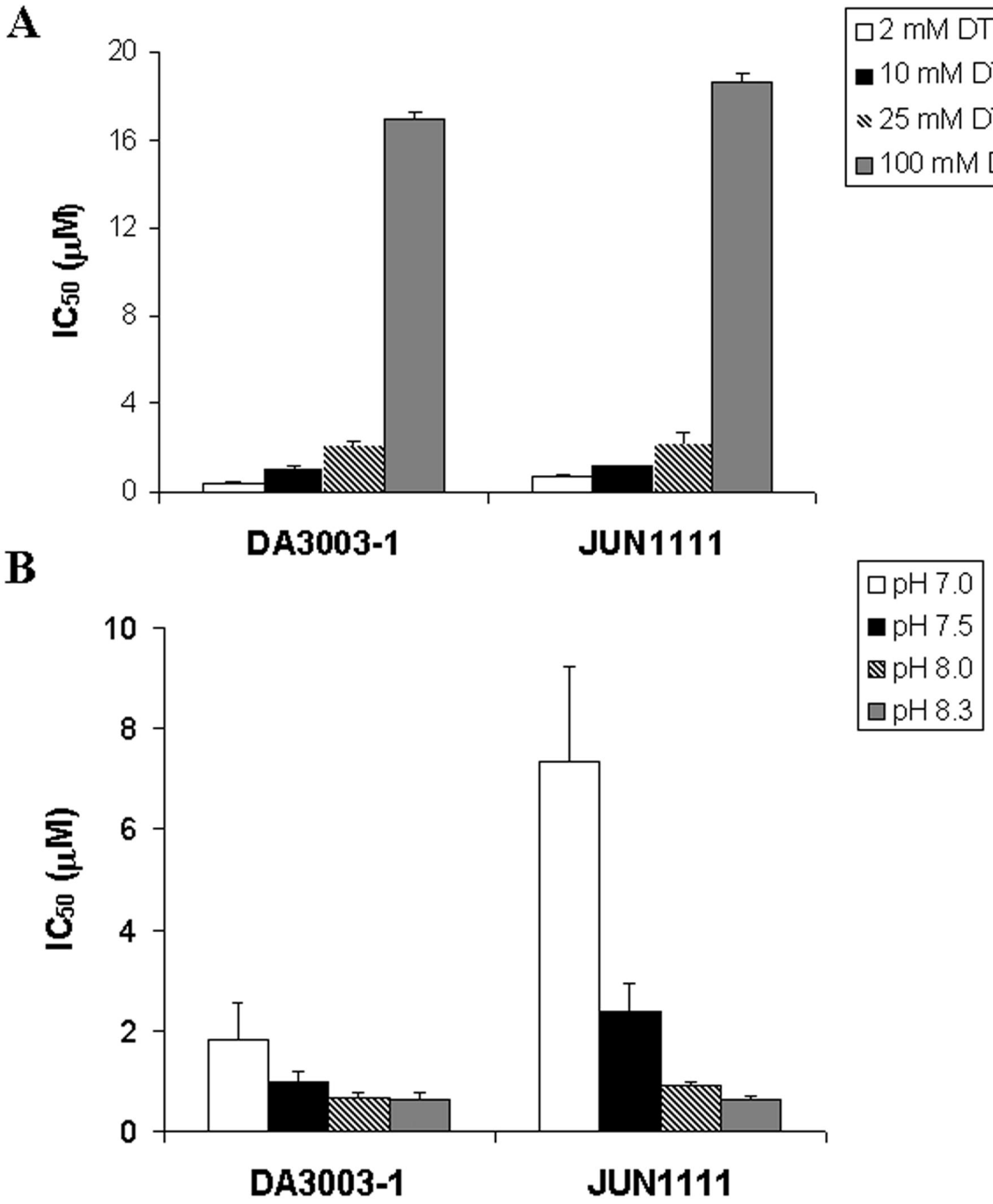

Figure 6

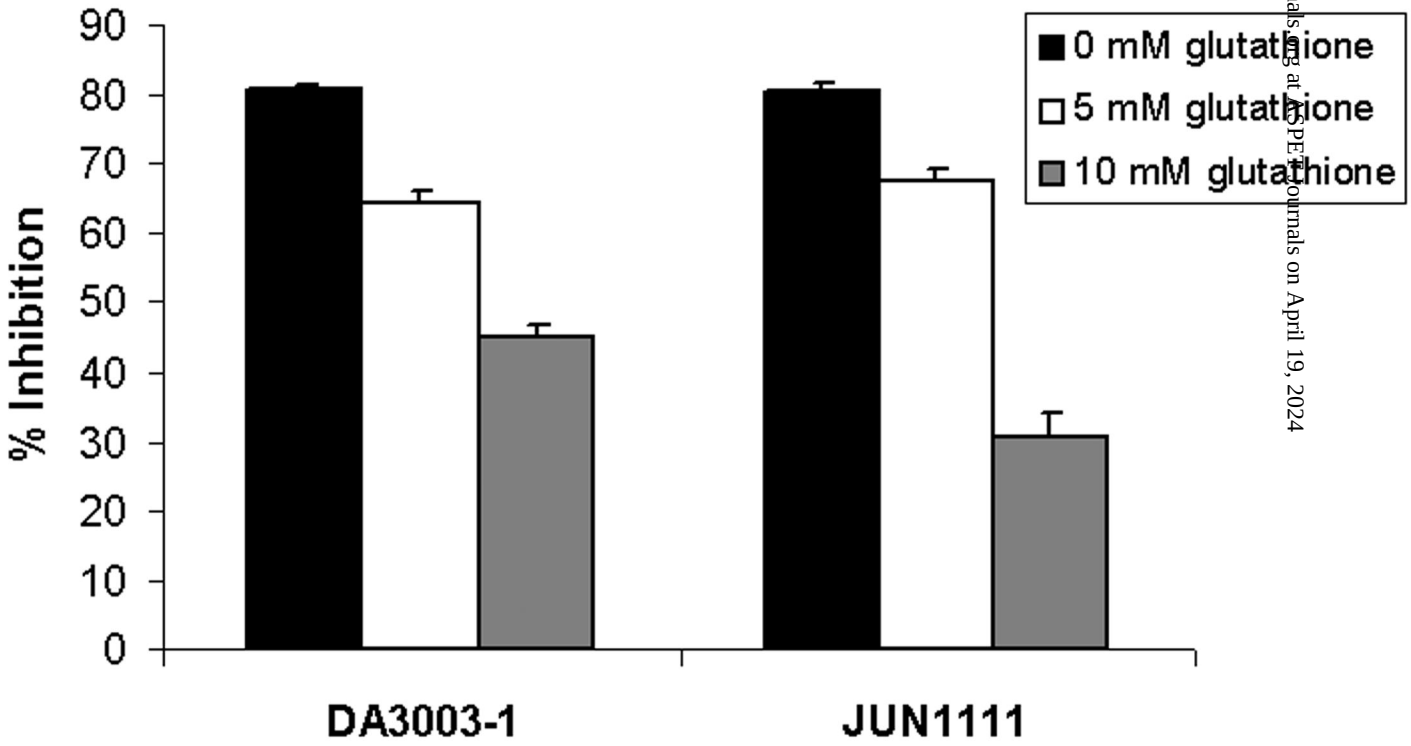

Figure 7

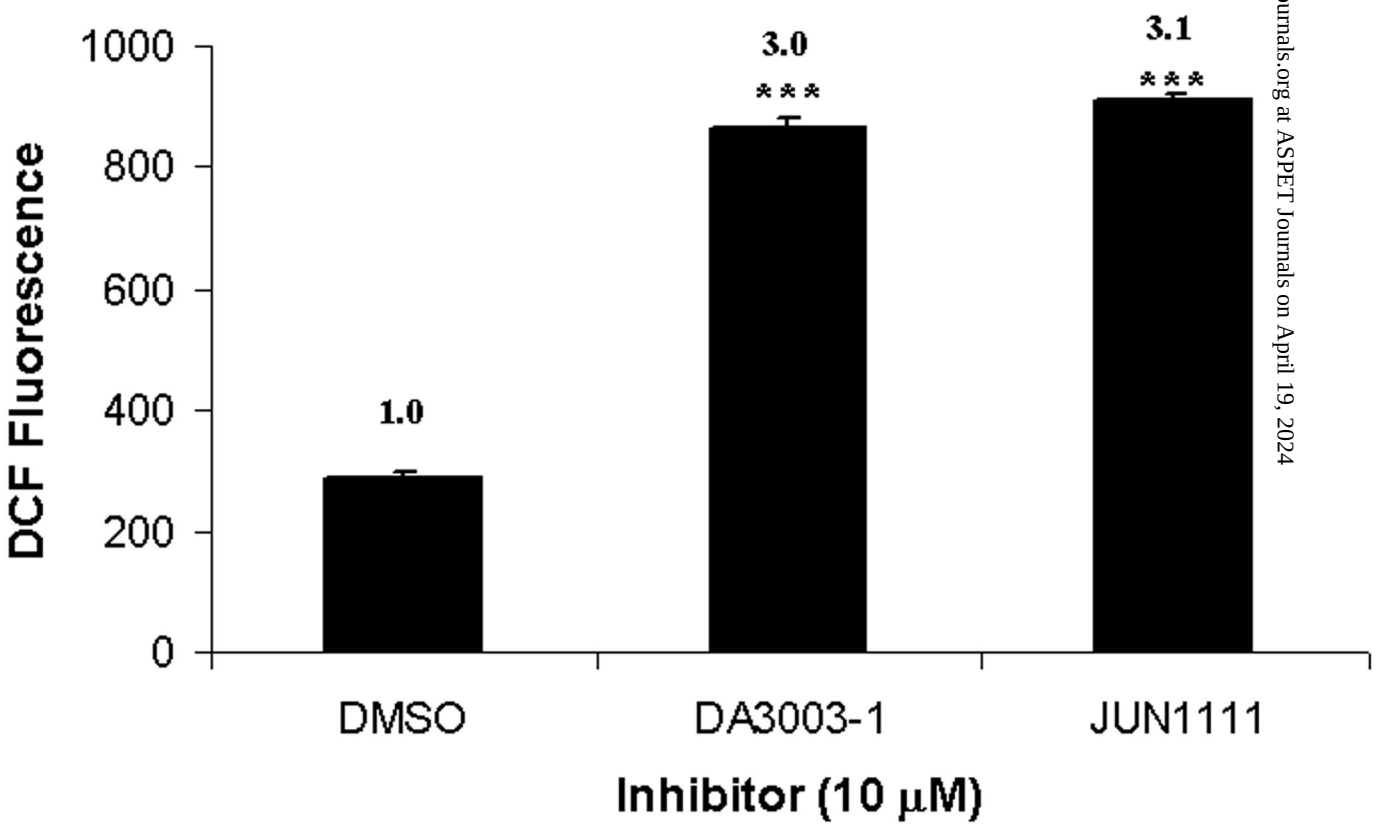

Figure 8

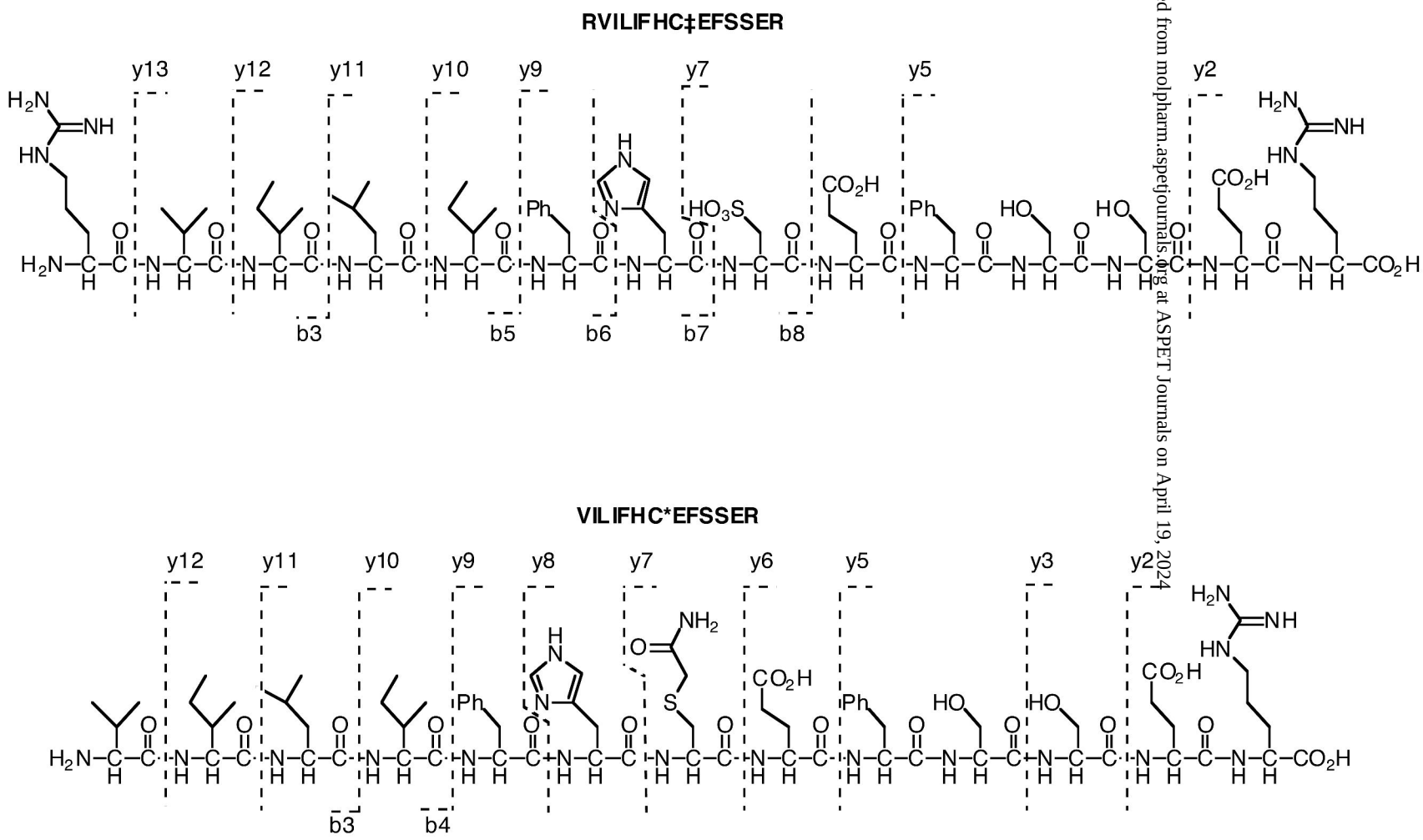

Figure 9